

Journal of Biomedical Optics

SPIEDigitalLibrary.org/jbo

Dynamic longitudinal investigation of individual nerve endings in the skin of anesthetized mice using *in vivo* two-photon microscopy

Mikhail Yuryev
Leonard Khiroug

Dynamic longitudinal investigation of individual nerve endings in the skin of anesthetized mice using *in vivo* two-photon microscopy

Mikhail Yuryev and Leonard Khiroug

University of Helsinki, Neuroscience Center, Viikinkaari 4, 00790 Helsinki, Finland

Abstract. Visualization of individual cutaneous nerve endings has previously relied on laborious procedures of tissue excision, fixation, sectioning and staining for light or electron microscopy. We present a method for non-invasive, longitudinal two-photon microscopy of single nerve endings within the skin of anesthetized transgenic mice. Besides excellent signal-to-background ratio and nanometer-scale spatial resolution, this method offers time-lapse “movies” of pathophysiological changes in nerve fine structure over minutes, hours, days or weeks. Structure of keratinocytes and dermal matrix is visualized simultaneously with nerve endings, providing clear landmarks for longitudinal analysis. We further demonstrate feasibility of dissecting individual nerve fibers with infra-red laser and monitoring their degradation and regeneration. In summary, our excision-free optical biopsy technique is ideal for longitudinal microscopic analysis of animal skin and skin innervations *in vivo* and can be applied widely in preclinical models of chronic pain, allergies, skin cancers and a variety of dermatological disorders. © 2012 Society of Photo-Optical Instrumentation Engineers (SPIE). [DOI: 10.1117/1.JBO.17.4.046007]

Keywords: two-photon microscopy; optical biopsy; skin innervation; cutaneous nerve endings; peripheral nervous system; *thy1* promoter; *thy1*-YFP-H mouse line.

Paper 11682L received Nov. 23, 2011; revised manuscript received Jan. 18, 2012; accepted for publication Feb. 1, 2012; published online Apr. 11, 2012.

1 Introduction

The various types of sensory nerve structures present in skin can be classified according to their modality as thermoreceptors, touch receptors and nociceptors.¹ Under physiological conditions, the number of sensory neurons innervating skin appears to be tightly regulated.² However, the dynamics of nerve endings can be significantly affected by different pathophysiological conditions.³ Indeed, changes in cutaneous nerves and nerve endings are involved in a variety of acute and chronic neurological disorders including traumatic injuries,⁴ Morton’s neuroma⁵ and peripheral neuropathies such as Meralgia Paraesthetica.⁶

Optical microscopy is a commonly used method for investigation of skin innervations. A major limitation of microscopic techniques is the necessity to excise skin tissue, fix it, prepare sections and apply markers and antibodies for histochemical and immunological staining. To allow tissue access for the antibodies during immunostaining in skin sheets *ex vivo*, mechanical separation of epidermis and dermis aided by chemical treatment has to be used.⁷ In addition to being tedious and literally painful to the patients, the *ex vivo* microscopic analysis fails to provide any information on the time course of the multiple dynamic processes which occur in skin under pathophysiological conditions. Thus, the invasiveness and lengthiness of the *ex vivo* procedures greatly hinders longitudinal measurements and renders analysis of nerve ending dynamics unfeasible.⁸

The introduction of transgenic mice expressing fluorescent proteins in specific neuronal subpopulations⁹ significantly broadened the possibilities of dynamical investigations by allowing

three-dimensional imaging of neuronal structures without additional staining.¹⁰ Application of transgenic mice has allowed long-term investigation of nerves in the skin.¹¹ However, structural measurements of sensory neurons have been restricted to *ex vivo* preparations. For instance, the *thy1*-YFP-H transgenic mice⁹ have been applied in the studies of axon regeneration¹² as well as Wallerian degeneration.¹³ While it is possible, in principle, to visualize neurons in the skin of living transgenic mice using conventional wide-field or confocal microscopy,^{9–11} the light scattering nature of skin greatly reduces the quality of images and light penetration depth, thus hindering investigation of fine neuronal structures.

Two-photon microscopy (also known as multiphoton laser-scanning microscopy) is a break-through technology in the field of optical imaging.¹⁴ By exploiting longer near-infrared wavelengths for non-linear excitation of fluorophores, two-photon microscopy dramatically reduces the undesirable effects of light scattering in thick tissues such as skin. Moreover, due to non-linear summation of the energy of two photons required for exciting a fluorophore, fluorescence is only emitted strictly from the focal point of the objective. This feature endows two-photon microscopy with the intrinsic optical scanning property and ensures excellent axial resolution while significantly decreasing phototoxicity. These advantages make the technique particularly suitable for measurements in living tissues, especially in skin. Besides working with extrinsic fluorophores (such as fluorescent proteins and organic dyes), two-photon microscopy can be used for investigation of skin’s endogenous chromophores.¹⁵ However, to the best of our knowledge, longitudinal *in vivo* microscopic imaging of cutaneous nerve endings

Address all correspondence to: Leonard Khiroug, University of Helsinki, Neuroscience Center, Viikinkaari 4, 00790, Helsinki, Finland. Tel: +358 45 635 2270; E-mail: leonard.khirug@helsinki.fi.

has not been documented so far. Here, we report a dynamic investigation of skin innervations *in vivo* by means of two-photon microscopy in transgenic thy1-YFP-H mouse model.

2 Materials and Methods

Transgenic mice expressing yellow fluorescent protein (thy1-YFP-H transgenic line were purchased from Jackson Laboratory (Bar Harbor, ME, USA). Mice at the age of 2 to 4 months were anesthetized by i.p. injection of the mixture of ketamine 0.08 mg per g body weight (Ketaminol, Intervet International) and xylazine 0.01 mg · g⁻¹ (Rompun, Bayer), with additional injections of the same anesthetic as necessary. Eye drops (Viscotears, Novartis Pharmaceuticals) were applied for protecting the eyes from dehydration. The body temperature during the experiments was closely monitored and maintained at 37°C using a heating pad (Supertech) placed under the mouse. The footpad was cleaned with ethanol and positioned on a metal bar. A drop of water was placed on the skin and covered with a microscope slide. The slide was attached to a metal bar with paper clips to stabilize the footpad for subsequent imaging.

The two-photon imaging of nerve fibers, as well as two-photon nanosurgery of selected nerves, was performed using the FluoView 1000 MP system (Olympus). The excitation light was generated by a mode-locked Ti:Sapphire Mai-Tai DeepSee femtosecond laser (Spectra Physics). The laser emission was focused onto the specimen by the objective lens XLPlan N 25X (Olympus). The laser wavelength of 950 nm was used for excitation of YFP. Fluorescence was collected through the beam-splitting cube in four separate channels: 1. 397 to 412 nm for autofluorescence detection and consequential spectral unmixing of possible “bleed-through” of autofluorescence into the YFP channel; 2. 450 to 480 nm for detection of second harmonic generation (SHG) signal for collagen fiber visualization; 3. 520 to 550 nm for imaging of YFP+ nerves; and 4. 580 to 630 nm for detection of both YFP fluorescence and autofluorescence of cornified layer of epidermis and of hair. In those cases where strong autofluorescence from hair was detected in the third channel (520 to 550 nm) and YFP fluorescence was partly detected in the fourth channel (580 to 630 nm), spectral unmixing was performed using ImageJ (<http://rsbweb.nih.gov/ij/>).

During the investigation of thin structures, images were acquired at the resolution of either 800 × 800 pixels or 1024 × 1024 pixels to obtain more detailed pictures. Axial step was varied between 1 and 5 μm according to the spatial resolution needed. The laser power was initially set at 100 mW but was varied from spot to spot, depending on optical properties of each skin spot, in order to obtain comparable fluorescence intensity between experiments. The images were processed off-line using Imaris software (Bitplane).

The laser lesions were produced using the same laser as used for image acquisition. First, a z-stack with a 5-μm vertical step was acquired to obtain three-dimensional (3D) reconstruction of the nerve fibers structure and select the x, y and z coordinates for the desired area of lesion. Second, a micro-lesion was produced by parking the laser beam at the chosen point and increasing the laser power from 100 to 1000 mW. The dose of laser exposure was limited by setting the shutter open time to 1 s. Finally, the laser power was decreased back to 100 mW, and a time-lapse series of 3D image stacks of the same site was acquired over a period of minutes to days after lesion for dynamic investigation of the consequences of laser microsurgery.

To enable longitudinal experiments with repetitive imaging of the same nerve ending over periods of days or weeks, we developed the following procedure. The carpal pad was visually identified and used as a reference point, with its coordinates stored for future reference. A nerve fiber of interest was first selected at low magnification and followed all the way to the nerve ending chosen for laser surgery and longitudinal imaging. The horizontal coordinates of the corresponding imaging field were stored in relation to the carpal pad coordinates, while the vertical coordinate was calculated from the uppermost level of epidermal autofluorescence {see Video 1 for illustration of spatial relationship between superficial epidermis, nerves and collagen (MPEG, 6.5 MB) [<http://dx.doi.org/10.1117/1.JBO.17.4.046007.1>]}. During each subsequent imaging session, the hind paw was repositioned the same way as in the first session. The carpal pad was visually identified and used as a zero point in the horizontal coordinate system. For setting the vertical coordinate, autofluorescence of superficial epidermis was used.

3 Results and Discussion

The footpad of a thy1-YFP-H mouse anesthetized with ketamine/xylazine was placed under the microscope objective as shown in Fig. 1(a), covered with a glass slide and secured with clips [Fig. 1(b)]. The fixation strength was set at a minimal level to ensure stable imaging while avoiding excessive pressure that may occlude blood flow in skin capillaries, which was visualized in pilot experiments (data not shown). The areas of interest were selected by identifying fluorescent YFP-positive structures that were visible under standard wide-field epifluorescence conditions [Fig. 1(c)]. The selective neuronal expression of YFP in the thy1-YFP-H mice has been thoroughly documented (see Ref. 9 and Jackson Laboratories webpage <http://jaxmice.jax.org/strain/003782.html>). Taking into account the published data, and considering that the non-hairy skin

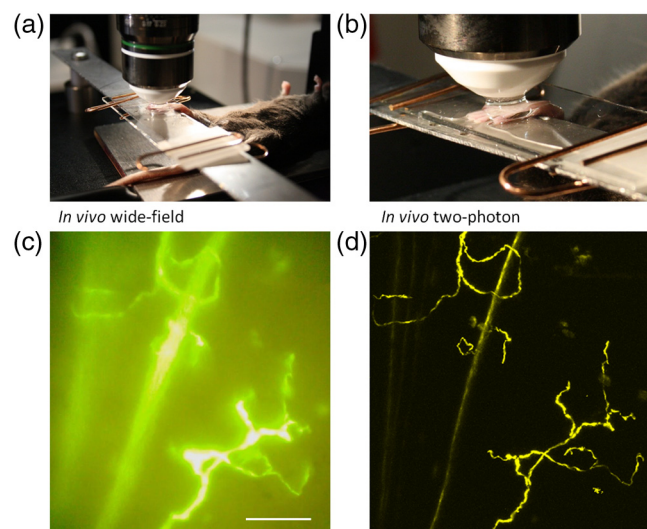


Fig. 1 Visualization of YFP+ nerves in the skin of mouse footpad. (a) Design of the two-photon imaging setup. The hind paw of the mouse with a drop of water on it is covered with a standard microscope slide to ensure optical coupling with a water-immersion objective. (b) Zoomed image of the mouse hind paw positioned in the set-up. (c) A wide-field epifluorescence image of nerve fibers in skin of the thy1-YFP-H mouse hind paw. Scale bar 100 μm. (d) Two-photon image of the same nerve fibers. See also Video 2 (MPEG, 8.0 MB) [<http://dx.doi.org/10.1117/1.JBO.17.4.046007.2>].

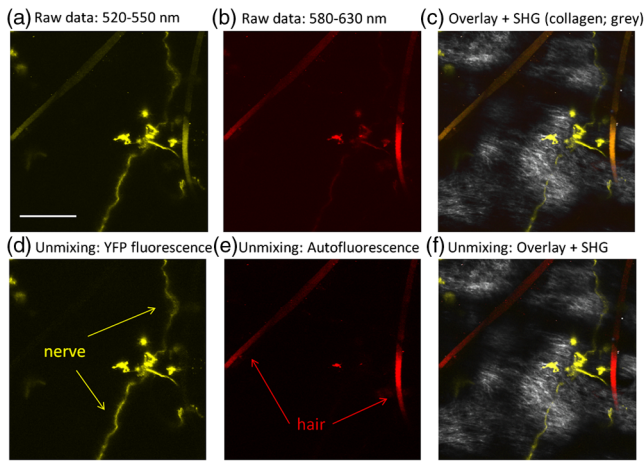


Fig. 2 Simultaneous detection of YFP fluorescence (yellow), hair autofluorescence (red) and Second Harmonic Generation (SHG) signal originating from collagen fibers (grey) shown as raw images prior to spectral unmixing (a, b, and c) and as processed images resulting from spectral unmixing (d, e, and f). Scale bar 100 μm .

regions of hind paw foot pad essentially lack motor neuron axons, we concluded that the YFP+ structures monitored in the present study were part of a small subset of sensory nerves originating from DRG neurons.^{9,16,17}

The z-stacks of optical sections were collected using two-photon excitation mode, and 3D projections were built revealing fine morphological details of YFP-positive nerve fibers and terminals [Fig. 1(d)]. For comparison, conventional wide-field image of the same region is shown in Fig. 1(c). Clear optical sections were obtained with two-photon microscopy at the depths of up to 250 μm (for animated projections of the image z-stack, see Video 2).

Fluorescence was collected using three separate emission channels. Emission of YFP fluorescence was collected in the spectral intervals of 520 to 550 nm [Fig. 2(a)] and 580 to 630 nm [Fig. 2(b)]. At the edges of footpad, YFP fluorescence occasionally partly overlapped with the autofluorescence of hair. Despite the overlapping spectra, it was possible to distinguish the nerve structures from hair and skin autofluorescence using mathematical unmixing routines¹⁸ [Fig. 2(d) and 2(e)]. Simultaneous collection of the second harmonic generation (SHG) signal and fluorescence of YFP [Fig. 2(c) and 2(f)] allowed us to investigate spatial distribution of neuronal network intertwined with collagen fibers, which would not be possible using conventional histological techniques.

Spatial relationship between nerve endings and collagen layers could be resolved as illustrated in Fig. 3(a) and Video 3. Thin structures that were situated in close proximity to each other could be clearly distinguished [Fig. 3(b)]. Full-width at half-maximum of the thinnest part of nerve is 750 ± 200 nm ($n = 5$) [Fig. 3(c)]. The fibers that were 3 μm apart from each other were fully discernible, as indicated by lack of overlap in their intensity profiles [Fig. 3(d)].

Moreover, it was possible to affect the nerves by producing selective lesions utilizing the same laser as for imaging (Fig. 4). To produce spatially restricted lesions to selected nerve fibers, we “parked” the laser beam at one spot to achieve continuous exposure of up to 500 ms. This technique allowed investigation of dynamic rearrangement of neuronal networks on a short time scale [Fig. 4(a) and 4(b)] as well as over the periods of days and weeks [Fig. 4(d) and 4(e)], potentially extendable to even longer periods of several months. Immediately after the lesion, the integrity of the targeted nerve fragment was lost and small structures resembling vesicles filled with YFP became clearly visible in the lesion area [Fig. 4(c)]. These round structures persisted for

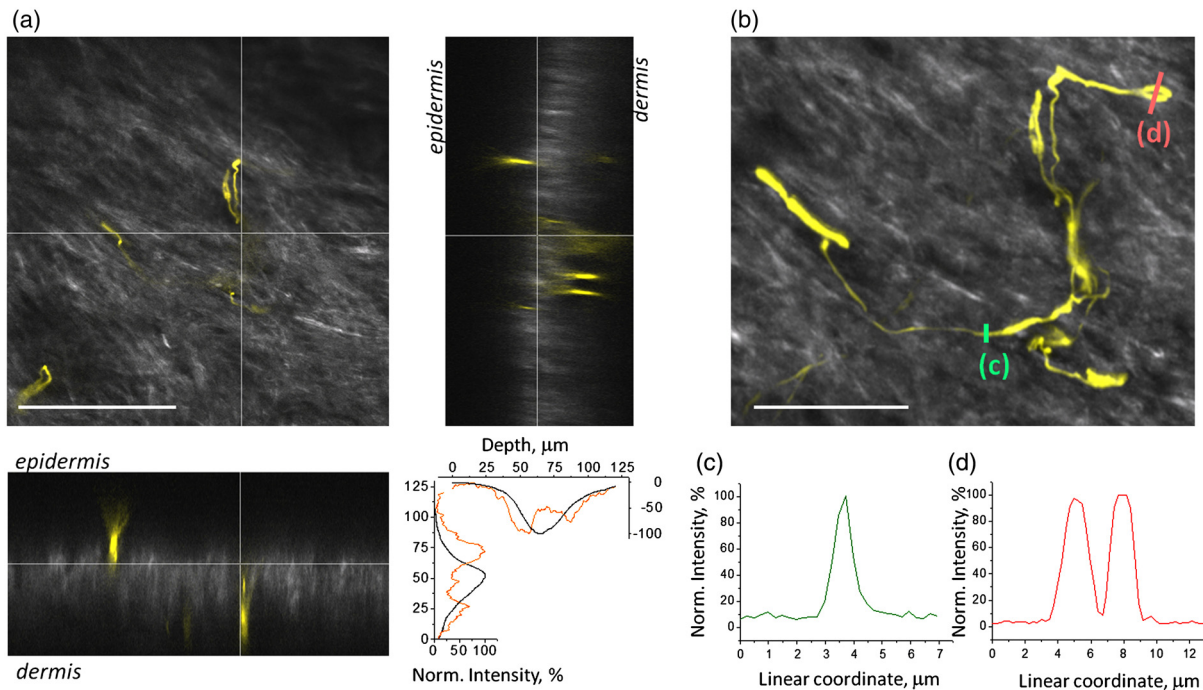


Fig. 3 Two- and three-dimensional image analysis. (a) Horizontal view of an optical section and the corresponding lateral projections of the YFP+ nerve fibers. The diagram shows normalized total intensity of the respective lateral projections. Scale bar 100 μm . (b) Zoomed maximum intensity projection of the z-stack. Scale bar 50 μm . Lines mark corresponding lateral intensity profiles of a single nerve fiber (c) and of two neighboring fibers (d). See also Video 3 (MPEG, 6.7 MB) [<http://dx.doi.org/10.1117/1.JBO.17.4.046007.3>].

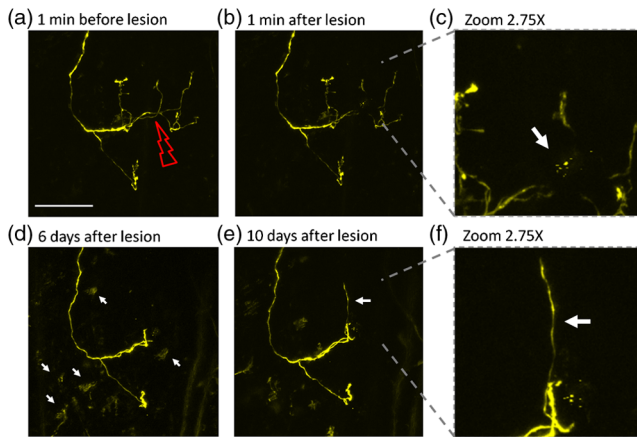


Fig. 4 Dynamic restructuring of cutaneous nerve endings induced by a local laser-mediated lesion. (a) Image of the nerves 1 min before the lesion. Arrow points to the area of damage. Scale bar 100 μm . (b) Image of the same spot 1 min after the lesion. (c) Zoomed area of the damage. Arrow points to the vesicles that have emerged around the site of injury. (d) The same region six days after the lesion. Arrows mark the diffusely fluorescent cell-size structures, presumably phagocytes. (e) The same region 10 days after the lesion. Arrow points on the newly developed nerve fiber. (f) Zoomed image of the emerging nerve fiber.

at least 10 days after the lesion [Fig. 4(d) and 4(e)], when re-innervation began as indicated by appearance of thin filopodia-like elongated YFP+ structures shown with an arrow in Fig. 4(e) and 4(f).

Interestingly, days later we observed diffuse cell-size structures with the spectral characteristics of YFP. It seems plausible to assume that these were phagocytes presumably participating in clearance of the severed nerve fibers. An alternative explanation is injury-induced transient expression of *thy1* in keratinocytes and subsequent *thy1*-driven expression of YFP in non-neuronal structures surrounding the severed nerve ending.¹⁰

“Nanosurgery,” or selective disruption of single axon has been demonstrated in the brain of anesthetized transgenic mice several years ago.¹⁹ However, the underlying physical principles of this process still remain elusive, especially in the case of its application to skin. The feasibility of producing highly selective lesions and disruptions of axons strongly depends on the scattering properties of the tissue. Typically, nerve endings that are positioned upon the collagen layer are more suitable for selective disruption. Although it is possible to produce lesions using shorter wavelength, e.g., 800 nm where YFP excitation is not optimal, precise disruption of single axons seems to be feasible only at the peak of YFP absorption at 950 nm (our unpublished observation).

After local injury the peripheral nerves may undergo significant regeneration or degradation. Insufficient functional recovery of nerve sensitivity after the sensory nerve injury remains an unmet clinical need. The incomplete re-innervation following the disruption of nerves may lead to abnormal sensory functions. The method presented here could be useful as an assay for developing new treatments for peripheral nerve injuries. It will be particularly interesting to investigate inflammatory processes concomitant to the nerve lesion by means of, for example, neutrophil staining *in vivo* via i.v. injection of antibodies.²⁰

There are several ways to circumvent physical limitations restricting optical investigations in skin. One of them is mounting of special skin fold chamber on the back of the animal to provide access to the deepest layers of skin for two-photon microscopic imaging.²¹ However, the skin fold chamber approach is more invasive compared to the method presented here. Another method providing access to the deep skin layers utilizes small-diameter fiber-optic probes that could provide real time images in the living animal, allowing access to peripheral nerve system as well as the brain. However, in addition to its invasive nature, the fiber-based method does not offer the spatial resolution required for investigation of subcellular structures.²²

Peripheral neuropathy remains an important clinical problem. This condition has been associated with a variety of disorders such as diabetes, immune diseases, drug toxicity (especially cancer chemotherapy) and HIV.⁸ Use of *in vivo* two-photon optical biopsy for morphological analysis in living transgenic mice will provide new and significant insights in these areas of research. Different lines of transgenic mice expressing, e.g., GFP, DsRed or CFP could be used in these types of experiments for convenient spectral separation.^{9,23} This is essential for experiments where, simultaneously with nerve endings, visualization of blood flow and extravasation of i.v.-injected tagged drug or blood plasma is desired. Using the mice with fluorescently marked mitochondria will enable functional imaging of nerve endings in skin. A promising and flexible approach is the *in vivo* electroporation, which allows expressing fluorescent proteins of interest in the nervous system of postnatal animals as we and others have previously shown.^{24,25}

In conclusion, we designed the protocol for single nerve endings visualization in *thy1*-YFP-H transgenic mice using two-photon microscopy. The method allows monitoring dynamic changes in thin structure of nerve fibers with submicron resolution over the periods of days or weeks.

Acknowledgments

This work was partly funded by the Academy of Finland. Mikhail Yuryev gratefully acknowledges the financial support and methodological training he received from Neurotar Ltd (www.neurotar.com) in the course of this project.

References

1. E. A. Lumpkin and M. J. Caterina, “Mechanisms of sensory transduction in the skin,” *Nature* **445**(7130), 858–865 (2007).
2. M. Koltzenburg, C. L. Stucky, and G. R. Lewin, “Receptive properties of mouse sensory neurons innervating hairy skin,” *J. Neurophysiol.* **78**(4), 1841–1850 (1997).
3. W. R. Kennedy, G. Wendelschafer-Crabb, and T. Johnson, “Quantitation of epidermal nerves in diabetic neuropathy,” *Neurology* **47**(4), 1042–1048 (1996).
4. L. R. Robinson, “Traumatic injury to peripheral nerves,” *Muscle Nerve* **23**(6), 863–873 (2000).
5. K. K. Wu, “Mortons’s interdigital neuroma: a clinical review of its etiology, treatment, and results,” *J. Foot Ankle Surg.* **35**(2), 112–119 (1996).
6. P. H. Williams and K. P. Trzil, “Management of meralgia paresthetica,” *J. Neurosurg.* **74**(1), 76–80 (1991).
7. E. Tschachler et al., “Sheet preparations expose the dermal nerve plexus of human skin and render the dermal nerve end organ accessible to extensive analysis,” *J. Invest. Dermatol.* **122**(1), 177–182 (2004).
8. G. Lauria and R. Lombardi, “Skin biopsy: a new tool for diagnosing peripheral neuropathy,” *BMJ* **334**(7604), 1159–1162 (2007).

9. G. Feng et al., "Imaging neuronal subsets in transgenic mice expressing multiple spectral variants of GFP," *Neuron* **28**(1), 41–51 (2000).
10. Y. A. Pan and J. R. Sanes, "Non-invasive visualization of epidermal responses to injury using a fluorescent transgenic reporter," *J. Invest. Dermatol.* **123**(5), 888–891 (2004).
11. C. Cheng et al., "Dynamic plasticity of axons within a cutaneous milieu," *J. Neurosci.* **30**(44), 14735–14744 (2010).
12. A. W. English, W. Meador, and D. I. Carrasco, "Neurotrophin-4/5 is required for the early growth of regenerating axons in peripheral nerves," *Eur. J. Neurosci.* **21**(10), 2646–2634 (2005).
13. B. Beirowski et al., "The progressive nature of Wallerian degeneration in wild-type and slow Wallerian degeneration (Wlds) nerves," *BMC Neurosci.* **6**, 6 (2005).
14. F. Helmchen and W. Denk, "Deep tissue two-photon microscopy," *Nat. Meth.* **2**(12), 932–940 (2005).
15. K. Koenig and I. Riemann, "High-resolution multiphoton tomography of human skin with subcellular spatial resolution and picoseconds time resolution," *J. Biomed. Opt.* **8**(3), 432–439 (2003).
16. M. L. Groves et al., "Axon regeneration in peripheral nerves is enhanced by proteoglycan degradation" *Exp. Neurol.* **195**(2), 278–292 (2005).
17. C. M. Webb, E. M. Cameron, and J. P. Soundberg, "Fluorescence-labeled reporter gene in transgenic mice provides a useful tool for investigating cutaneous innervation," *Vet. Pathol.* 21 July 2011, (2011).
18. T. Zimmermann et al., "Spectral imaging and linear un-mixing enables improved FRET efficiency with a novel GFP2-YFP FRET pair," *FEBS Lett.* **531**(2), 245–249 (2002).
19. L. Sacconi et al., "In vivo multiphoton nanosurgery of cortical neurons," *J. Biomed. Opt.* **12**(5), 050502 (2007).
20. M. Phillipson et al., "Intraluminal crawling of neutrophils to emigration sites: a molecularly distinct process from adhesion in the recruitment cascade," *J. Exp. Med.* **203**(12), 2569–2575 (2006).
21. F.-C. Li et al., "Dorsal skin fold chamber for high resolution multiphoton imaging," *Opt. Quant. Elect.* **37**(13), 1439–1445 (2005).
22. P. Vincent et al., "Live imaging of neural structure and function by fibred fluorescence microscopy," *EMBO Rep.* **7**(11), 1154–1161 (2006).
23. T. Mischak et al., "Imaging axonal transport of mitochondria in vivo," *Nat. Methods* **4**, 559–561 (2007).
24. C. Boutin et al., "Efficient in vivo electroporation of the postnatal rodent forebrain," *PLoS One* **3**(4), e1883 (2008).
25. D. Molotkov et al., "Gene delivery to postnatal rat brain by non-ventricular plasmid injection and electroporation," *J. Vis. Exp.* **43**, 2244 (2010).